JOURNAL OF VIROLOGY, Nov. 1997, p. 8750–8758 Vol. 71, No. 11
0022-538X/97/$04.00+0

Evolutionary Variants of the Human Immunodeficiency Virus Type 1 V3 Region Characterized by Using a Heteroduplex Tracking Assay

JULIE A. E. NELSON,[1] SUSAN A. FISCUS,[2] AND RONALD SWANSTROM[1,3]*

Lineberger Comprehensive Cancer Center,[1] Department of Microbiology and Immunology,[2] and Department of Biochemistry and Biophysics,[3] University of North Carolina at Chapel Hill, Chapel Hill, North Carolina 27599

Received 10 April 1997/Accepted 18 August 1997

Syncytium-inducing (SI) variants of human immunodeficiency virus type 1 (HIV-1) are evolutionary variants that are associated with rapid CD4$^+$ cell loss and rapid disease progression. The heteroduplex tracking assay (HTA) was used to detect evolutionary V3 variants by amplifying the V3 sequences from viral RNA derived from 50 samples of patient plasma. For this V3-specific HTA (V3-HTA), heteroduplexes were formed between the patient V3 sequences and a probe with the subtype B consensus V3 sequence. Evolution was then measured by divergence from the consensus. The presence of evolutionary variants was correlated with SI detection data on the same samples from the MT-2 cell culture assay. Evolutionary variants were correlated with the SI phenotype in 88% of the samples, and 96% of the SI samples contained evolutionary variants. In most cases the evolutionary V3 variants represented discrete clonal outgrowths of virus. Sequence analysis of the six discordant samples that did not show this correlation indicated that three non-syncytium-inducing (NSI) samples had V3 sequences that had evolved away from the consensus sequence but not toward an SI genotype. A fourth sample showed little evolution away from the consensus but was SI, which indicates that not all SI variants require basic substitutions in V3. The other two samples had SI-like genotypes and NSI phenotypes, suggesting that V3-HTA was able to detect SI emergence in these samples in the absence of their detection in vitro. V3-HTA was also used to confirm SI variant selection in MT-2 cells and to examine the possibility of variant selection during virus culture in peripheral blood cells.

The rapid evolution of human immunodeficiency virus type 1 (HIV-1) in infected individuals is due to high replication rates (24, 49), error-prone replication (39), and selective pressure exerted by the host's immune system (33). Several types of variants, which can be distinguished by their in vitro phenotypes, can emerge over the course of infection. Syncytium-inducing (SI) variants of HIV-1 are able to induce syncytium formation in a transformed T-cell line called MT-2, and their presence in peripheral blood mononuclear cells (PBMC) or plasma has been correlated with rapid disease progression (28, 46). SI variants are only rarely transmitted; instead they evolve de novo in 50% of infected individuals from a non-syncytium-inducing (NSI), macrophage-tropic parent (45). When SI variants are transmitted, the onset of AIDS is very rapid, typically within 2 years of infection (47). It is not known what role SI variants play in rapid progression, although it has been suggested that they may be more than bystanders, since the plasma viral load increases after the emergence of SI variants (10). Not all individuals who show rapid progression have SI variants, however, which suggests that the SI phenotype in vitro does not fully explain the phenomenon of rapid progression.

The SI phenotype is one of many traits along a continuum of HIV-1 phenotypes. The SI phenotype is usually linked with rapid replication rates to high titers, the ability to infect transformed T-cell lines, and the loss of the ability to infect macrophages (2). It is not known, however, whether all these characteristics are conferred by the same determinants that give the SI phenotype. Tropism is determined by the ability of the virus to bind to both CD4 and a specific chemokine coreceptor. CCR5 and CXCR4 are the chemokine receptors used most commonly by HIV-1, with CCR5 usage associated with macrophage-tropic viruses and CXCR4 usage associated with T-cell-line-tropic viruses (15, 18, 19). Many primary SI viruses have been found to be dual tropic, in that they can infect both macrophages and transformed T-cell lines. As expected, dual-tropic viruses are able to use either receptor for infection, and some of the viruses can use other chemokine receptors as coreceptors (9, 17, 44). However, coreceptor usage does not completely define tropism. Cheng-Mayer et al. and others were unable to show a strict correlation between macrophage tropism and usage of the CCR5 coreceptor (5, 16). The linkage between tropism and phenotype is also unclear. Because a transformed T-cell line is used to test for the SI phenotype, SI variants must be either T-cell line tropic or dual tropic. But the NSI phenotype does not predict tropism, since Chesebro et al. found that there are separate determinants for NSI phenotype and macrophage tropism (8). Schuitemaker et al. described five different viral classifications based on isolates from different time points of infection that had different tropisms and NSI or SI phenotypes (42). Given that the cell type supporting replication in vivo is not known, the meaning of these in vitro correlates of phenotype remains uncertain.

Studies of the SI phenotype have focused on the determinants required to switch from NSI to SI. All of the determinants for NSI or SI phenotype and tropism are in the *env* gene, with most of them in the third variable (V3) domain of gp120. V3 contains the primary neutralization epitope of gp120 (27) and is, therefore, under high selective pressure from the immune system. Recombinant and mutagenesis studies of sub-

* Corresponding author. Mailing address: 139 Lineberger Comprehensive Cancer Center, CB#7295, University of North Carolina at Chapel Hill, Chapel Hill, NC 27599. Phone: (919) 966-5710. Fax: (919) 966-3015. E-mail: risunc@med.unc.edu.

type B viruses have identified many different amino acid substitutions that can contribute both to the SI phenotype and to a switch in tropism, although none of the changes is found in all SI variants (6–8, 11, 22, 25, 38, 43, 50). An accumulation of basic amino acids in the V3 domain, especially at positions 11, 24, 25, and 32, is the most common feature of SI variants (21, 34). Also, the V3 regions of SI variants have approximately twice as much variation (beyond the basic amino acid substitutions) as NSI V3 regions compared to a consensus sequence (7, 34).

The heteroduplex mobility assay (HMA) and the heteroduplex tracking assay (HTA) were developed to examine the divergence in HIV *env* sequences within individuals and between populations by using PCR products that included V3 (13, 14). The assays are based on the observation that DNA heteroduplexes migrate through polyacrylamide more slowly than do DNA homoduplexes due to kinks formed by the unpaired bases (3). HMA examines all of the heteroduplexes formed by analysis of ethidium bromide-stained gels, while HTA is used to visualize only the heteroduplexes that form between a radioactively labeled probe and the driver PCR products. By using nested PCR to amplify a 700-bp region including V3, Delwart et al. showed that the complexity of viral variants in PBMC DNA from an infected individual could be visualized by HMA (13). Shifts in mobility were shown to depend on the extent of divergence between the two strands of the heteroduplex: the greater the divergence, the slower the migration of the heteroduplex.

In this report we describe a rapid genotype-based assay for the detection of evolutionary variants of V3. The assay involves the amplification of V3 sequences from viral RNA isolated from patient plasma, followed by analysis of the V3 sequences by HTA to determine whether evolutionary variants are present in the patient plasma sample. The heteroduplex patterns were found to be reproducible and represented the sequence variants in the plasma samples. The V3 sequences from 50 patients were analyzed by using V3-specific HTA (V3-HTA), and the results were compared with the NSI or SI phenotype determined in MT-2 cell culture. V3-HTA was able to detect 96% of MT-2 cell-tropic, SI variants as evolutionary V3 variants and overall showed an 88% correspondence in identifying SI and NSI viruses. Further examination of the viruses that were discordant between the MT-2 cell culture assay and V3-HTA has revealed novel HIV-1 variants, with an example of an SI virus without basic substitutions in V3 and two NSI viruses with basic substitutions usually associated with the SI phenotype. In addition, V3-HTA has been used to document the selection of SI variants in MT-2 cells and to show the potential for selection during culture of virus in peripheral blood cells.

MATERIALS AND METHODS

Patient samples. All samples used in this study were obtained as excess tissue samples with institutional review board approval. Blood samples were collected from the patients through the AIDS Clinical Trial Units at the University of North Carolina at Chapel Hill, Duke University, and Georgetown University or from patients attending the Infectious Disease Clinic at the University of North Carolina at Chapel Hill.

Cells, plasma, and virus culture. Blood from patients was collected in acid-citrate-dextrose tubes. After centrifugation at 800 × *g* for 20 min, cell-free plasma was aliquoted and frozen at −70°C. PBMC were isolated on Ficoll-Hypaque gradients and cocultured with phytohemagglutinin-stimulated PBMC from uninfected donors in quantitative HIV cultures as described previously (20, 37). Excess PBMC were frozen as viable cells in freezing medium containing dimethyl sulfoxide as described previously (37). After 2 weeks in culture, virus from the cocultures was tested in triplicate for syncytium formation in MT-2 cells by using a previously described method (26, 37). Virus isolates from each positive PBMC culture were stored at −70°C. In a few cases these frozen virus stocks were used to confirm the presence or absence of SI isolates in MT-2 cell cultures. Supernatants from some of these MT-2 and PBMC cultures were also tested by V3-HTA.

Plasmids and vectors used. Plasmid pUC112-1, a *Sac*I subclone of JR-FL, was generously provided by Irvin Chen, University of California, Los Angeles (29). The NL4-3 V3 sequence was amplified from a subclone of the NL4-3 genomic molecular clone (1). Plasmids B-NSI and B-SI are clones generated from a PCR product from PBMC genomic DNA derived from patient B, described by Milich et al. (34); the PCR products were cloned into the pCRII TA vector (Invitrogen). The JR-FL probe plasmid pJN27 was made by cloning the 141-bp V3 PCR product from pUC112-1 into pCRII. The downstream *Eco*RI site was destroyed by partially digesting the plasmid with *Eco*RI, filling in the overhangs with the Klenow fragment of DNA polymerase I, and recircularizing the plasmid. Reverse transcription (RT)-PCR products were cloned into the pT7Blue TA vector (Novagen). After transformation of the ligations into DH5α bacteria, the white colonies were screened by colony PCR (31) followed by HTA as described below. Plasmids were sequenced by using Sequenase 2.0 (U.S. Biochemicals). Sequences were manipulated with Wisconsin Package version 9.0 (Genetics Computer Group, Madison, Wis.).

RNA isolation and RT-PCR. Thawed plasma or supernatant (0.5 to 1.0 ml) from PBMC coculture was spun in a Beckman TL-100 ultracentrifuge with a TL-55S rotor at 45,000 rpm for 15 min. The virus pellet was resuspended in 140 μl of plasma or phosphate-buffered saline. Supernatant from MT-2 cells was used without centrifugation. Viral RNA was isolated from the 140 μl of virus by using a QIAamp Viral RNA kit (Qiagen), which gave a final volume of approximately 50 μl. Primers for RT-PCR were 5′-GAATCTGTAGAAATTAATTGTACAAGACCC-3′ (V3L4) and 5′-TTTTGCTCTACTAATGTTACAATGTGCTTG-3′ (V3R5). RT-PCR was performed as follows. Ten-microliter RT reactions consisted of 5 μl of viral RNA, 1× Perkin-Elmer PCR buffer II (50 mM KCl, 10 mM Tris [pH 8.3]), 5 mM $MgCl_2$, 1 mM each deoxynucleoside triphosphate (dNTP) (U.S. Biochemicals), 15 pmol of primer V3R5, 10 U of RNase inhibitor (Perkin-Elmer Corp.), and 25 U of Moloney murine leukemia virus reverse transcriptase (Perkin-Elmer). RT was done at 42°C for 30 min, followed by 10 min at 99°C to inactivate the reverse transcriptase. Forty microliters of PCR master mix (1× PCR buffer II, 2.5 mM $MgCl_2$, 15 pmol of primer V3L4, 1.25 U of Perkin-Elmer Ampli*Taq* polymerase) was then added to the RT reaction mixtures. PCR was carried out in either a Perkin-Elmer TC1 thermal cycler (95°C for 3 min; 95°C for 10 s, 48°C for 10 s, 72°C for 20 s, 40 cycles) or a Stratagene Gradient-40 Robocycler (96°C for 3 min; 96°C for 45 s, 51°C for 45 s, 72°C for 45 s, 40 cycles). PCRs with plasmids were done by using the same cycle conditions with the following reaction components: 1× PCR buffer II, 2.5 mM $MgCl_2$, 0.1 μM each primer, 10 pg of plasmid, and 1.25 U of Ampli*Taq* polymerase. RT-PCR amplifications were repeated for higher efficiency of amplification with Boehringer Mannheim enzymes in a method modified from their Titan one-tube RT-PCR system. Twenty-microliter RT reaction mixtures consisted of 1 to 5 μl of viral RNA, 1× Titan RT-PCR buffer, 2.5 mM $MgCl_2$, 5 mM dithiothreitol, 0.5 mM each dNTP, 15 pmol of primer V3R5, 10 U of RNase inhibitor (Perkin-Elmer), and 12 U of avian myeloblastosis virus reverse transcriptase (Boehringer Mannheim). RT was done at 42°C for 30 min, and the enzyme was inactivated at 99°C for 2 min. Thirty microliters of PCR mix (1× RT-PCR buffer, 2.5 mM $MgCl_2$, 5 mM dithiothreitol, 15 pmol of primer V3L4, and 2.6 U of Expand High Fidelity enzyme mix [Boehringer Mannheim]) was then added to the RT reaction mixtures. PCR was done in the Stratagene Robocycler with the following program: 95°C for 2 min 45 s; 95°C for 45 s, 51°C for 45 s, 68°C for 1 min, 40 cycles (after the first 10 cycles, 1 min was added to the 68°C step for 10 cycles, 2 min was added for the next 10 cycles, and 3 min was added for the last 10 cycles). PCR products were sequenced by using the ABI PRISM dye terminator cycle sequencing kit (Perkin-Elmer).

HTA. The JR-FL V3 probe was labeled by first digesting 1.5 μg of plasmid pJN27 with *Eco*RI. A total of 1.25 μCi of α-^{35}S-dATP (1,250 Ci/mmol; NEN Life Science Products) and 2 U of the Klenow fragment of DNA polymerase I were added to the digest for 15 min, followed by heat inactivation of the enzymes. The plasmid was further digested with *Pst*I to remove the probe from the vector, and the probe was then purified by using QIAquick PCR purification columns (Qiagen) to give a final volume of 50 μl. Heteroduplex formation reactions were done as described by Delwart et al. (14) with the following modifications. The reactions consisted of 1 μl of 10× annealing buffer (1 M NaCl, 100 mM Tris-HCl [pH 7.5], 20 mM EDTA), 8 μl of unpurified PCR product, 0.1 μM primer V3L4, and labeled JR-FL probe to make 10 μl. Primer V3L4 was included in the heteroduplex formation reactions to normalize for PCRs containing excess primer after amplification. The reactions were denatured at 95°C for 2 min and allowed to anneal at room temperature for 5 min. The heteroduplexes were separated in 12% acrylamide (37.5:1, acrylamide:bisacrylamide) gels in 1× TBE buffer (41). A model V16-2 vertical gel apparatus (Gibco BRL) was used, and the gels were run at 17 mA (per gel) until the xylene cyanol dye had run off the bottom of the gel (approximately 6 h). The gels were dried and analyzed by using either autoradiography with X-ray film or phosphor imaging screens (Molecular Dynamics).

Nucleotide sequence accession numbers. The V3 nucleotide sequences reported here have been assigned GenBank accession no. AF001798 to AF001827.

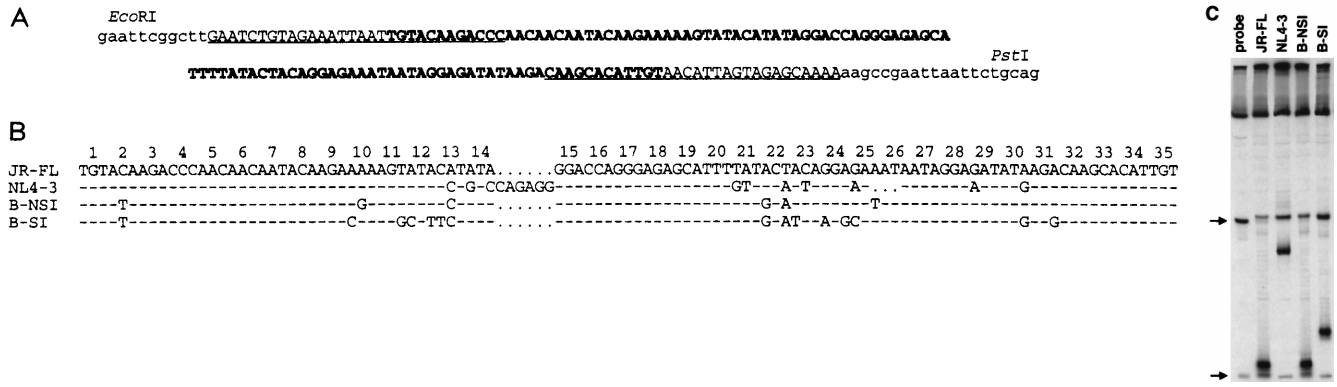

FIG. 1. (A) Probe for SI detection by V3-HTA. The V3 region PCR product (shown in capital letters) from the pUC112-1 subclone of JR-FL was cloned into the pCRII TA vector. The primers (described in Materials and Methods) that were used to amplify V3 from plasmids and viral RNA are underlined. The *Eco*RI and *Pst*I sites were used to excise the probe from the vector. The V3 coding region is shown in bold; lowercase letters indicate additional sequences derived from the vector that are part of the probe. (B) V3 sequence alignment of the clones used for V3-HTA. JR-FL and B-NSI are NSI-like; NL4-3 and B-SI are SI-like. The amino acids of V3 are numbered starting with the first cysteine of V3 as 1. All sequences are compared with JR-FL; dashes represent the same nucleotide as in the JR-FL sequence, while dots represent deletions. (C) Autoradiogram of V3-HTA gel. The arrows designate the single-stranded probe (top) and the probe homoduplex (bottom). The lane labeled "probe" contains only probe in a heteroduplex reaction.

RESULTS

SI and NSI sequences can be distinguished by an HTA directed to the V3 coding region. HTA is able to distinguish between heteroduplexes based on the number of mismatches between the probe sequence and the test sequence (13). Because the changes in the V3 coding region of HIV-1 *env* that lead to the SI phenotype differ widely among isolates, HTA is ideal for SI detection. Previous applications of HTA employed PCR products between 350 and 1,200 bp, typically spanning sequences from V3 to V5 (12, 14). Because the difference in variability that distinguishes SI and NSI variants is largely confined to V3, we designed two 30-nucleotide primers to amplify a 141-bp PCR product, of which 81 bp are target dependent and within V3. The V3 sequence from the macrophage-tropic NSI molecular clone JR-FL was chosen for use as the probe in the heteroduplex reactions because it is nearly identical to the consensus sequence for subtype B (36). SI sequences on average have twice as much variation in sequence from the consensus as do NSI sequences, in addition to the accumulation of basic amino acid substitutions (34). Therefore, this probe should be different from most SI sequences and more similar to most NSI sequences in patients infected with subtype B HIV-1, making the SI heteroduplexes distinguishable from the NSI heteroduplexes. The probe was constructed by amplifying the 141-bp region from the pUC112-1 molecular clone of JR-FL (29) and ligating the PCR product into a TA vector. By using a cloned fragment rather than labeling during PCR, greater consistency in probe preparation was achieved. A second probe-containing plasmid was made by eliminating one of the *Eco*RI sites flanking the insert to allow radioactive end labeling of only one strand by filling in the remaining *Eco*RI overhang with a labeled nucleotide (Fig. 1A).

In order to test our ability to differentiate between homogeneous NSI and SI sequences by using the JR-FL V3 probe and V3-HTA, V3 region sequences were amplified from molecular clones of known sequence. These clones included JR-FL (control) and NL4-3 (SI) subclones and two clones (B-NSI and B-SI) generated from a patient whose lymphocytes harbored both NSI- and SI-like V3 sequences (34). Figure 1B shows a comparison of the sequences of the clones used. The PCR product from each clone was mixed with probe labeled on one or both strands, denatured, and annealed to form heteroduplexes. The heteroduplexes were separated in a polyacrylamide gel, producing sample-specific migration patterns. Gels containing 12% acrylamide produced the optimal distinction between the two types of sequences, and probes labeled on only one strand produced the clearest patterns for interpretation. Adding denaturant (15% urea [12]) to the gel caused smearing of some of the slower-migrating SI bands, which made the bands less prominent. The probe labeled on both strands usually formed twice the number of distinct heteroduplex species as the probe labeled on just one strand, since the two strand-specific heteroduplexes that form with each product usually migrate differently (not shown). Figure 1C shows the mobility patterns of the PCR products annealed with the probe labeled on one strand. The single-stranded probe and the double-stranded probe homoduplex are both seen in all lanes. The bands at the top of the gel are labeled vector fragments. All heteroduplexes formed between the probe and PCR products run more slowly (i.e., are higher in the gel) than the probe homoduplex, even when the PCR product is from JR-FL; this is because the probe has short extensions on both ends derived from the plasmid. This slightly greater length produces tails on each of the heteroduplexes that slow their mobility in polyacrylamide slightly. Therefore, any bands that are above the probe homoduplex band are scored as heteroduplexes in this assay.

The NSI and SI heteroduplexes migrated very differently, demonstrating that V3-HTA can distinguish these NSI and SI sequences. The JR-FL and B-NSI sequences produced heteroduplexes with fast mobility (close to the probe homoduplex), while the NL4-3 and B-SI sequence heteroduplexes were much slower, with the NL4-3 heteroduplex close to the single-stranded probe band. The NL4-3 sequence has fewer mismatches with the JR-FL sequence than does B-SI, but it has a 6-bp insertion as well as a 3-bp deletion. These types of changes have large effects on the mobility of the heteroduplexes (48). The B-NSI heteroduplex shows that an NSI sequence with five differences in sequence from JR-FL (within the target-dependent 81 bp) still migrates like an NSI sequence and is distinguishable from the B-SI sequence. Thus, the assay does not measure total variability but rather distinctive features of V3 sequence evolution associated with the SI phenotype (see below).

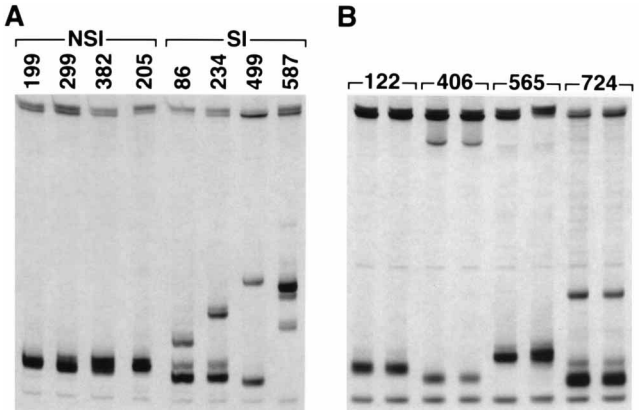

FIG. 2. (A) Examples of V3-HTA patterns for 8 of the 50 patient plasma samples. The NSI and SI designations refer to the phenotypes determined by MT-2 cell culture assay. (B) V3-HTA of duplicate, independent RT-PCRs for each RNA sample. Only the bottom halves of the gels are shown; for descriptions of the top and bottom bands in each lane, see the legend to Fig. 1.

Comparison between V3-HTA and the MT-2 cell culture assay for SI detection. In order to test the effectiveness of V3-HTA in detecting SI variants in patients, plasma samples from 50 patients were tested by V3-HTA. The detection of evolutionary variants by V3-HTA was compared with the phenotypes determined by the MT-2 cell culture assay as a measure of V3-HTA efficiency. The MT-2 cell culture assay used virus generated by coculture of the patients' infected PBMC with phytohemagglutinin-stimulated PBMC from uninfected donors. The infected PBMC were taken from the same blood samples as the plasma used for V3-HTA. Plasma samples were chosen so that about half of the samples were from patients harboring SI variants as measured by the MT-2 cell culture assay.

Viral RNA was isolated from the plasma, and RT-PCR was performed to generate V3 PCR products for V3-HTA. Figure 2A shows representative results from the V3-HTA gels. Heteroduplex patterns are shown for four NSI plasma samples that did not have V3 evolutionary variants and four SI plasma samples that had V3 evolutionary variants. The latter lanes show examples of the variety of heteroduplex patterns seen in SI plasma samples. The heteroduplex patterns showed a surprising degree of homogeneity in the viral pools, even among many of the patient plasma samples with SI variants. As the representative heteroduplex patterns in Fig. 2A show, the patient plasma samples with V3 evolutionary variants can have greater complexity (more bands) overall than those without, but most of these samples had only one or two major variants. This analysis confirms earlier observations, based on PBMC DNA, that viral outgrowths are largely clonal (30, 34). The V3-HTA results also agree with the observation that viral sequences tend to be more homogeneous early in infection and more heterogeneous late in infection (32). The variability that is seen among patients suggests that V3-HTA is a sensitive assay for genotypic differences among the SI variants that evolve independently in each individual.

In an attempt to assess whether the V3-HTA patterns were reproducible, several of the patient plasma samples that had multiple bands in the V3-HTA were amplified in triplicate and V3-HTA was done on all of the products. The same patterns were obtained with all products from a single RNA sample, some of which are shown in Fig. 2B. In addition, consecutive plasma samples (within 2 months) were obtained from a few of the patients. The V3-HTA patterns of these later plasma samples were the same in heteroduplex pattern and intensity (not shown), indicating that the V3 sequence heteroduplex patterns were reproducible and were representative of the sequences in the patients' blood at the time of collection. These results are in agreement with the reproducibility of HTA patterns seen by Delwart et al. (13), who showed that their patterns were reproducible when there was high DNA input in their first round of nested PCR. Since we were not using nested PCR on these viral RNA samples, our reproducibility results show that we were using a sufficient amount of input RNA to get proper sampling of the variants present. We have not yet established limits on the reproducibility of the assay under conditions of low virus load.

The mobility of the slowest (highest in the gel) heteroduplex for each of the 50 patient plasma samples was measured (distance from the well in centimeters) and divided by the mobility of the probe homoduplex to produce a heteroduplex mobility ratio that was compared among samples. The heteroduplex mobility ratios are shown graphically with the MT-2 cell culture phenotypes in Fig. 3. The V3-HTA results were optimally grouped by drawing a line at 0.91 to separate the majority of the NSI and SI samples. Samples above the line had V3 evolutionary variants, and samples below the line did not. Because of the small sample size in this study, the line may be subject to a small change as the assay continues to be tested. Of the 27 patient plasma samples that had the SI phenotype in MT-2 cells, 26 had V3 evolutionary variants that formed heteroduplexes with mobility ratios of less than 0.91, while 18 of the 23 MT-2 NSI samples did not. This is an overall concordance of 88% (with 6 of 50 samples discordant between the two assays) and 96% concordance in identifying SI patient samples by detection of V3 evolutionary variants in plasma virus.

The majority of V3 variants present in a patient's plasma are detected by V3-HTA. It is possible that V3-HTA does not show the correct heteroduplex pattern for a patient's viral pool if the majority of variants in a patient's blood are diverse and each is at low abundance. This possibility was tested by analyzing individual clones of the PCR products from each of two patient plasma samples, 300 and 717. The V3-HTA patterns for these plasma samples are shown in Fig. 4A. The clones were sequenced (Fig. 5A) and analyzed by V3-HTA beside the patient plasma PCR product (not shown) to connect each sequence with a specific heteroduplex band from the patient plasma sample; heteroduplex bands were numbered starting from those closest to the top of the gel.

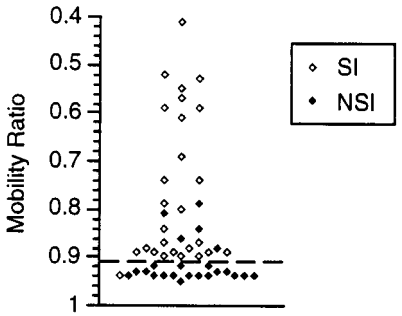

FIG. 3. Mobility ratios determined from V3-HTA were plotted with the MT-2 cell phenotype for each of the 50 patient plasma samples tested. Mobility ratios were calculated by dividing the migration distance of the top heteroduplex by the migration distance of the probe homoduplex. The dashed line at 0.91 designates the maximum mobility ratio for a positive score for the presence of V3 evolutionary variants. For comparison, the mobility ratio for the JR-FL control PCR product was 0.96.

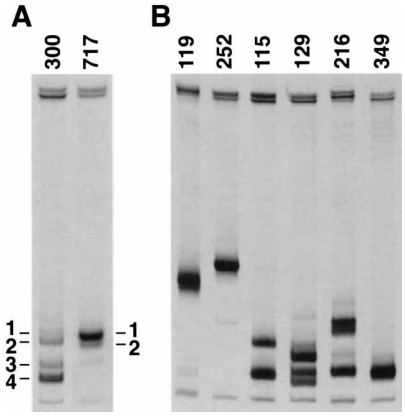

FIG. 4. (A) V3-HTA of patient plasma samples 300 and 717. The positions of the heteroduplexes generated with each patient sample are shown and numbered starting with the most slowly migrating species. (B) V3-HTA of the six discordant patient plasma samples that did not show a correlation between MT-2 cell phenotype and detection of V3 evolutionary variants by V3-HTA.

All of the clones analyzed matched in mobility one of the bands from the patient plasma sample RNA, indicating that the heteroduplex patterns accurately displayed the variants present in the plasma. The 38 clones from patient plasma sample 300 included 18 with the same NSI-like sequence that had the mobility of the darkest band in the V3-HTA (Fig. 4A, band 4). Several other clones had similar sequences and the same mobility. There were nine clones corresponding to band 2, which represented the major SI-like variant in this individual, while bands 1 and 3 were represented by one and three clones, respectively. Similar results were obtained with patient sample 717. The percentage of clones corresponding to each band is shown in Table 1, as is the relative percentage by intensity of each of the bands on the V3-HTA gel. The percentages are similar, indicating that clone screening is consistent with the pattern of variants as detected by V3-HTA. The discrepancies in absolute values between the numbers are likely due to the small numbers of clones examined.

For patient plasma sample 300, the clone from band 1 had only one more substitution than the clones from band 2, while many of the clones in band 4 differed by a single substitution without a shift in mobility. Also, two clones from sample 300 with six substitutions each had different mobilities (bands 3 and 4). These results show that HTA does not differentiate heteroduplexes solely by the number of mismatches. We have concluded, therefore, that V3-HTA is more sensitive to mismatch clustering than to the total number of mismatches.

Patient plasma samples with discordant phenotypes identified differences between V3-HTA and the MT-2 cell culture assay. The six patient plasma samples with discordant phenotypes were examined further to determine why they did not show a correlation between SI phenotype and the presence of V3 evolutionary variants. Figure 4B shows the heteroduplex patterns for the discordant patient samples. To ensure that the patient PBMC were not misscored for syncytium formation in the initial MT-2 cell culture assay, the discordant samples were

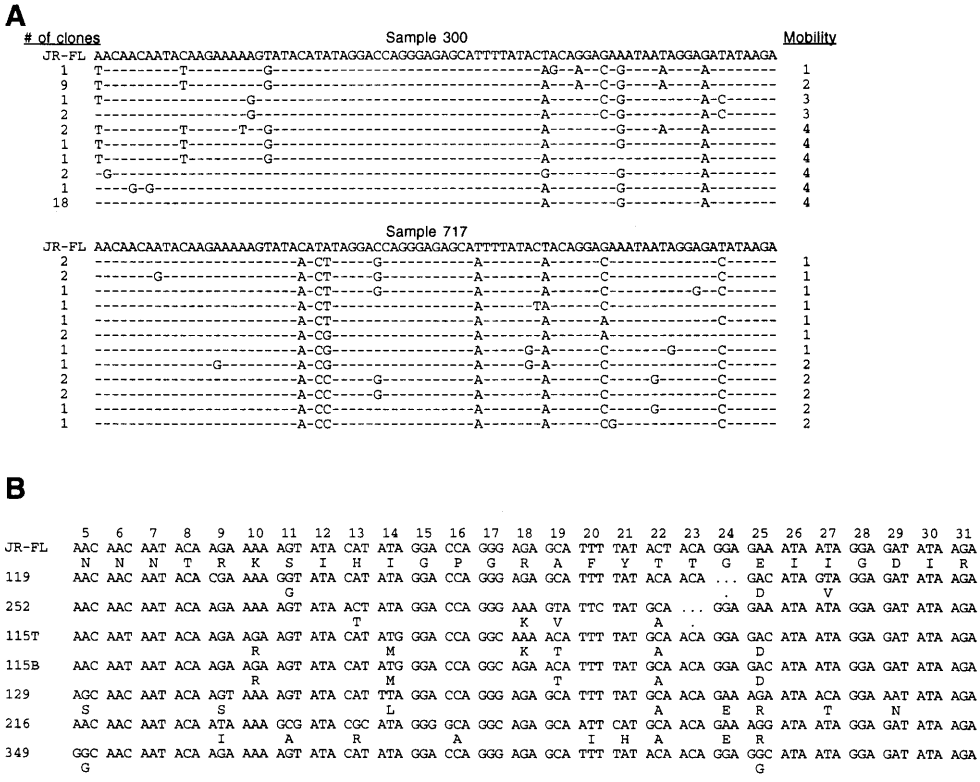

FIG. 5. (A) V3 sequence alignment of individual clones of variants from patient plasma samples 300 and 717. In both groups, the sequences are compared with the sequence of JR-FL to highlight mismatches in heteroduplexes. Dashes represent the same nucleotide as shown in the JR-FL sequence. The number of clones isolated with the given sequence is shown, as is the mobility of each sequence as determined by V3-HTA. Heteroduplex bands shown in Fig. 4 were numbered from the top. (B) V3 nucleotide and predicted amino acid sequence alignment of the variants from the six discordant patient plasma samples. The numbering of V3 begins with the first cysteine as amino acid 1. Only predicted amino acids that differ from JR-FL are shown; dots represent deletions.

TABLE 1. Percentages of variants with specific mobilities from cloned RT-PCR products and relative intensities of heteroduplex bands in V3-HTA

Gel band[a]	% Clones with same mobility[b]	% Band intensity by V3-HTA[c]
300-1	2	8.5
300-2	24	17.5
300-3	8	21
300-4	66	53
717-1	59	85
717-2	41	13.5
717-3	0	1.5

[a] Heteroduplex gel bands are numbered from the top.
[b] Percentage of clones that had the same mobility as the corresponding HTA gel band. Thirty-eight clones were sequenced from patient sample 300, and seventeen clones were sequenced from patient sample 717.
[c] Percentage by intensity for each band in V3-HTA as calculated by area integration with ImageQuant software (Molecular Dynamics).

retested from frozen viral isolates obtained from the initial coculture. In all cases, the phenotype of the PBMC coculture virus was confirmed.

The RT-PCR products from two discordant samples with homogeneous PCR products were sequenced using an automated sequencing machine. Patient samples 119 and 252, which had V3 evolutionary variants but did not cause syncytia in MT-2 cells, each had a 3-bp deletion in the V3 sequence that caused the heteroduplex shift (Fig. 5B). Thus, these sequences have NSI-like genotypes and NSI phenotypes, with a small deletion that indicates V3 evolution by V3-HTA. In these cases, direct sequence analysis of the homogeneously shifted PCR products explained the discordance between V3-HTA and the MT-2 assay. Therefore, discordance between the assays can be reduced in future applications by sequencing all homogeneous PCR products that have heteroduplex shifts to discover whether there are deletions or insertions.

Three clones of the RT-PCR product from patient plasma sample 349, which did not have V3 evolutionary variants but induced syncytia in MT-2 cells, encoded no basic amino acid substitutions in their V3 regions, although each one did encode a substitution to glycine at position 25. To verify that this variant was responsible for the SI phenotype, viral RNA was isolated from the medium supernatants of the PBMC coculture and MT-2 cell infection of patient sample 349. RT-PCR was performed on the viral RNA, and the heteroduplex patterns were compared with the pattern from the plasma sample. In the PBMC coculture and MT-2 cell supernatants, just as in the plasma, only the single fast-migrating heteroduplex was present. The sequence of the RT-PCR product from the MT-2 cell supernatant was the same as the sequence of the plasma RT-PCR product, indicating that this variant is able to induce syncytia in vitro despite a lack of SI-associated amino acid substitutions within V3.

For discordant patient samples that had heterogeneous viral pools and therefore could not be sequenced directly from the PCR product, the PCR products were cloned and then screened by V3-HTA to identify clones that had the same mobility as the sequences of interest. The sequences of these clones are shown in Fig. 5B. Patient samples 115, 129, and 216 had V3 evolutionary variants but did not induce syncytia in MT-2 cells. The sequences of the two heteroduplex variants from patient plasma sample 115 show that there is only a one-nucleotide difference between them despite a large mobility shift. Both variants had many substitutions, although none of the substitutions are associated with the SI phenotype. The added nucleotide substitution in the top variant produced a cluster of mismatches with the JR-FL probe, causing the shift in mobility of this variant heteroduplex. The sequences of the top heteroduplexes from patient plasma samples 129 and 216 showed that these variants had several SI-associated substitutions, including basic substitutions in both cases. However, these changes are apparently insufficient for syncytium induction in MT-2 cells. Longitudinal studies of patients are required to determine if sequence variants like these represent precursors to SI variants, pathogenic variants that do not induce syncytia in MT-2 cells, or NSI variants.

Analysis of the variants produced by PBMC coculture and MT-2 cell infection and comparison to variants present in plasma. In our comparison of V3-HTA of plasma RNA to the MT-2 cell culture assay for the ability to detect SI variants, the two assays could be detecting completely different virus populations. It is not known where in the body SI and NSI viruses are produced, so the virus in the plasma could be unrelated to the virus produced by coculture of patient PBMC. Also, selection may occur for certain variants during PBMC coculture and minor variants could be selected in the subsequent MT-2 cell infection. Selection of sequence variants has been previously shown to occur during culture of PBMC from some patients (40). In that study, viral *tat* and *env* sequences were compared among plasma, uncultured PBMC DNA, and virus that grew out of cultured PBMC, demonstrating that PBMC culture sometimes produced only subsets of the sequences present in the plasma or uncultured PBMC. V3-HTA is a convenient way to address the question of selection in PBMC and MT-2 cells by comparing the virus populations in these cells with the virus population in plasma.

Supernatants containing cell-free virus from PBMC coculture and MT-2 cell infections were collected for 15 patient samples that were SI in MT-2 cell culture. The heteroduplexes corresponding to plasma, PBMC coculture, and MT-2 cell infection from the same patient sample were compared by V3-HTA, and three different types of heteroduplex patterns were observed. The first type, seen in patient samples 622 and 476 (Fig. 6), had the same heteroduplex pattern from all viral sources. This type was observed for three other patient samples. Only one heteroduplex was seen for patient sample 622, indicating that the plasma variant detected by V3-HTA was the variant that caused syncytia in MT-2 cells. Patient sample 476 had two heteroduplexes, indicating that both variants were

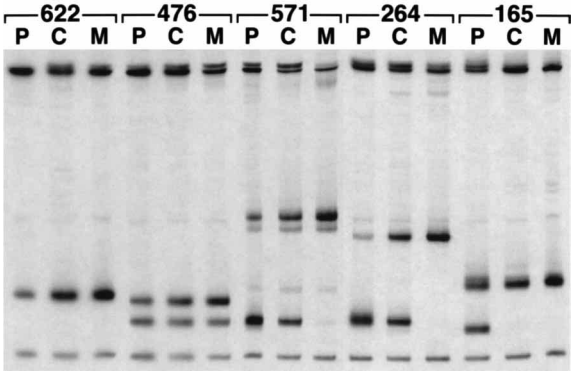

FIG. 6. V3-HTA comparison of variants present in plasma (P), PBMC coculture medium (C), and MT-2 cell medium (M), all derived from the same patient blood samples (shown above the lanes).

able to infect MT-2 cells and that at least one of them was able to induce syncytia.

In the second type of heteroduplex pattern, several variants were detected but selection in MT-2 cells was apparent. One of the variants in plasma and PBMC coculture from patient sample 571 was not present in the virus from MT-2 cells. For patient sample 264 (Fig. 6) and five others (not shown), the same variants were detected in plasma and PBMC coculture but the relative abundance of the variants was different between plasma and PBMC coculture. In the case of patient sample 264, the higher variant that was more abundant in the PBMC coculture was the one that induced syncytia. Therefore, this variant was SI, fast replicating, and different from the subtype B V3 consensus sequence while the lower variant was NSI and slow replicating.

The third type of heteroduplex pattern had a difference between the number of variants detected from plasma and that detected from PBMC coculture. This type was seen for patient sample 165 (Fig. 6) and two others (not shown). In the case of patient sample 165, the plasma had an additional lower heteroduplex that would be scored as NSI by V3-HTA. Because this variant did not appear in PBMC coculture, selection may have occurred there. Alternatively, the change in pattern could have been due to the lack of the lower heteroduplex variant in the PBMC if it was produced by noncirculating cells, such as macrophages or tissue lymphocytes. From these results, we conclude that in most cases, V3-HTA identifies the same variants that emerge from PBMC coculture for MT-2 cell test infection. For some samples, however, the variants that grow out of PBMC coculture are only a subset of the variants found in the plasma.

DISCUSSION

V3-HTA is a rapid genotype-based assay that is able to detect evolutionary V3 variants of HIV-1 in samples of patient plasma. In an analysis by V3-HTA of 50 plasma samples from patients, 31 contained evolutionary V3 variants. The association between the presence of evolutionary variants and SI variants in patient samples was determined by comparing the results of V3-HTA with the SI or NSI phenotypes from the MT-2 cell culture assay. V3-HTA indicated the presence of evolutionary variants in 96% of the samples that were SI in MT-2 cells. Overall, V3-HTA results predicted the presence or absence of SI variants in 88% of the samples. The heteroduplex patterns showed clonal outgrowth of variants in patient plasma, which is in agreement with previous observations, based on the analysis of patient PBMC DNA, that several distinct populations of virus appear to coexist (30, 34). In our studies, many of the SI samples had only evolutionary variants that corresponded to the SI phenotype, which suggests that NSI variants were either replaced or overgrown by SI variants in these individuals. In other SI samples, there were several V3 evolutionary variants. In the one case where we examined the sequence relationships among the multiple variants, some sequences appeared to be intermediate to the evolution of others (sample 300) (Fig. 5A). We reached a similar conclusion in studying the PBMC DNA of two previous patients (34).

Through the comparison of V3-HTA and sequence analysis, two conclusions can be made about the physical basis for the shifts seen in V3-HTA. First, deletions and insertions that produce shifts in heteroduplex mobility are not necessarily associated with SI phenotypes and do not necessarily have the hallmarks of SI genotypes. Deletions of 3 bp resulted in large heteroduplex shifts in this use of HTA, as is seen when larger PCR products are used (13). Patient plasma samples 119 and 252 each had a 3-bp deletion that was completely responsible for the large shift in mobility but apparently did not affect the phenotype. Second, shifts in heteroduplex mobility do not reflect the total number of mismatches in the heteroduplex but rather the placement of the mismatches. Delwart et al. showed that heteroduplex mobility is slowed with an increasing percentage of mismatches (without deletions) in the heteroduplex (13). In V3-HTA, however, clustering of at least two mismatches no more than 1 bp apart appears to be necessary for a shift in mobility. The sequences of the two variants from patient plasma sample 115 showed that a single-substitution difference was sufficient for a shift in mobility, since that substitution formed a cluster of three mismatches, spaced 1 bp apart, in the heteroduplex. Sequences of variants from patient plasma sample 300 confirmed the clustering effect on heteroduplex shifts. Two different clones from sample 300 each had six substitutions, but the mobilities of the heteroduplexes from these clones were different. The clone that had two mismatches that were only 1 bp apart had a shift to lower mobility compared to the clone with an equivalent number of widely spaced mismatches.

Sequence analysis provided explanations for the discordance between SI phenotype and the presence of evolutionary V3 variants for six of the patient plasma samples studied. As discussed above, two of the NSI samples had 3-bp deletions within their NSI V3 sequences that resulted in heteroduplex shifts in V3-HTA. The sequence of the PCR product from a third sample, 115, that was NSI in MT-2 cells showed that this patient's virus had evolved away from the NSI consensus but was not evolving toward an SI phenotype. Because of the wide variety of V3 sequences that have been identified among individuals infected with subtype B HIV-1, it is expected that a few variant V3 sequences (like those from patients 115, 119, and 252) will have sufficient mismatches with the consensus probe to produce V3-HTA shifts while remaining NSI. For two other discordant patient samples, 129 and 216, evolutionary variants were detected by V3-HTA and the sequences of the PCR products from plasma had changes associated with SI genotypes but the PBMC-derived virus was NSI. These results suggest that evolution toward SI may be occurring in these individuals, which would indicate that V3-HTA is able to detect the development of SI variants prior to their detection in MT-2 cells. Alternatively, these sequences may be different types of variants that are not evolving toward the SI phenotype. These variants may still be biologically relevant and may even lead to rapid progression but fail to score in the MT-2 cell culture assay. The sequence of the single SI patient sample, 349, that did not have evolutionary variants in V3-HTA showed no SI-associated substitutions in V3. Thus, for this variant, the SI determinants must lie outside of V3. SI determinants have been identified outside of V3, although usually these determinants are required in addition to V3 substitutions (4, 23).

As described above, V3-HTA measures clustering of mismatches in heteroduplexes rather than the total number of mismatches. This feature of the assay is actually advantageous for detection of SI variants. The NSI variants in different infected individuals can vary greatly from the NSI consensus while remaining NSI. Since the scattered mutations typically seen in these NSI V3 sequences do not cause shifts in heteroduplex mobility, few plasma samples will produce a false score in V3-HTA. On the other hand, SI variants tend to have a greater amount of variability, especially around positions 19 to 25 (35), which results in clustered mismatches. Therefore, V3-HTA is especially well suited to the differentiation between NSI and SI variants.

The sequence analysis of these patient samples with discor-

dant phenotypes in the two assays indicated that the assays had different sensitivities. By definition, the MT-2 cell culture assay is able to detect SI variants, but it is an assay for an in vitro phenotype. It is not known whether the ability of a variant to induce syncytia in MT-2 cells is directly related to a biological consequence of HIV infection. Therefore, it is possible that people who have rapid disease progression may have variants that are important in disease but do not cause syncytia in MT-2 cells. V3-HTA, on the other hand, detects variation within V3. The assay is able to detect variants that may be biologically relevant in terms of disease course, regardless of their ability to infect or induce syncytia in MT-2 cells. The assay may also be able to detect the evolution toward SI before the MT-2 cell culture assay does, which could be used to identify patients in whom therapy could possibly prevent SI emergence.

ACKNOWLEDGMENTS

This work was supported by grant 9513-ARG-0019 from the North Carolina Biotechnology Center (R.S.) and by Adult ACTG developmental contract 96VD006 from the National Institutes of Health (S.A.F.). J.A.E.N. was supported by postdoctoral training grant T32-CA-09156 from the National Cancer Institute.

We thank Irvin Chen for plasmid pUC112-1. We also thank Ada Cachafeiro, Qing Yang, and Amie Miano for technical assistance.

REFERENCES

1. **Adachi, A., H. E. Gendelman, S. Koenig, T. Folks, R. Willey, A. Rabson, and M. A. Martin.** 1986. Production of acquired immunodeficiency syndrome-associated retrovirus in human and nonhuman cells transfected with an infectious molecular clone. J. Virol. **59:**284–291.
2. **Asjo, B., J. Albert, A. Karlsson, L. Morfeldt-Manson, G. Biberfeld, K. Lidman, and E. M. Fenyo.** 1986. Replicative properties of human immunodeficiency virus from patients with varying severity of HIV infection. Lancet **ii:**660–662.
3. **Bhattacharyya, A., and D. M. Lilley.** 1989. The contrasting structures of mismatched DNA sequences containing looped-out bases (bulges) and multiple mismatches (bubbles). Nucleic Acids Res. **17:**6821–6840.
4. **Carrillo, A., and L. Ratner.** 1996. Human immunodeficiency virus type 1 tropism for T-lymphoid cell lines: role of the V3 loop and C4 envelope determinants. J. Virol. **70:**1301–1309.
5. **Cheng-Mayer, C., R. Liu, N. R. Landau, and L. Stamatatos.** 1997. Macrophage tropism of human immunodeficiency virus type 1 and utilization of the CC-CKR5 coreceptor. J. Virol. **71:**1657–1661.
6. **Chesebro, B., J. Nishio, S. Perryman, A. Cann, W. O'Brien, I. S. Y. Chen, and K. Wehrly.** 1991. Identification of human immunodeficiency virus envelope gene sequences influencing viral entry into CD4-positive HeLa cells, T-leukemia cells, and macrophages. J. Virol. **65:**5782–5789.
7. **Chesebro, B., K. Wehrly, J. Nishio, and S. Perryman.** 1992. Macrophage-tropic human immunodeficiency virus isolates from different patients exhibit unusual V3 envelope sequence homogeneity in comparison with T-cell-tropic isolates: definition of critical amino acids involved in cell tropism. J. Virol. **66:**6547–6554.
8. **Chesebro, B., K. Wehrly, J. Nishio, and S. Perryman.** 1996. Mapping of independent V3 envelope determinants of human immunodeficiency virus type 1 macrophage tropism and syncytium formation in lymphocytes. J. Virol. **70:**9055–9059.
9. **Choe, H., M. Farzan, Y. Sun, N. Sullivan, B. Rollins, P. D. Ponath, L. Wu, C. R. Mackay, G. LaRosa, W. Newman, N. Gerard, C. Gerard, and J. Sodroski.** 1996. The beta-chemokine receptors CCR3 and CCR5 facilitate infection by primary HIV-1 isolates. Cell **85:**1135–1148.
10. **Connor, R. I., H. Mohri, Y. Cao, and D. D. Ho.** 1993. Increased viral burden and cytopathicity correlate temporally with CD4+ T-lymphocyte decline and clinical progression in human immunodeficiency virus type 1-infected individuals. J. Virol. **67:**1772–1777.
11. **De Jong, J.-J., A. de Ronde, W. Keulen, M. Tersmette, and J. Goudsmit.** 1992. Minimal requirements for the human immunodeficiency virus type 1 V3 domain to support the syncytium-inducing phenotype: analysis by single amino acid substitution. J. Virol. **66:**6777–6780.
12. **Delwart, E. L., M. P. Busch, M. L. Kalish, J. W. Mosley, and J. I. Mullins.** 1995. Rapid molecular epidemiology of human immunodeficiency virus transmission. AIDS Res. Hum. Retroviruses **11:**1081–1093.
13. **Delwart, E. L., H. W. Sheppard, B. D. Walker, J. Goudsmit, and J. I. Mullins.** 1994. Human immunodeficiency virus type 1 evolution in vivo tracked by DNA heteroduplex mobility assays. J. Virol. **68:**6672–6683.
14. **Delwart, E. L., E. G. Shpaer, J. Louwagie, F. E. McCutchan, M. Grez, H. Rübsamen-Waigmann, and J. I. Mullins.** 1993. Genetic relationships determined by a DNA heteroduplex mobility assay: analysis of HIV-1 *env* genes. Science **262:**1257–1261.
15. **Deng, H., R. Liu, W. Ellmeier, S. Choe, D. Unutmaz, M. Burkhart, M. P. Di, S. Marmon, R. E. Sutton, C. M. Hill, C. B. Davis, S. C. Peiper, T. J. Schall, D. R. Littman, and N. R. Landau.** 1996. Identification of a major co-receptor for primary isolates of HIV-1. Nature **381:**661–666.
16. **Dittmar, M. T., A. McKnight, G. Simmons, P. R. Clapham, R. A. Weiss, and P. Simmonds.** 1997. HIV-1 tropism and co-receptor use. Nature **385:**495–496.
17. **Doranz, B. J., J. Rucker, Y. Yi, R. J. Smyth, M. Samson, S. C. Peiper, M. Parmentier, R. G. Collman, and R. W. Doms.** 1996. A dual-tropic primary HIV-1 isolate that uses fusin and the beta-chemokine receptors CKR-5, CKR-3, and CKR-2b as fusion cofactors. Cell **85:**1149–1158.
18. **Dragic, T., V. Litwin, G. P. Allaway, S. R. Martin, Y. Huang, K. A. Nagashima, C. Cayanan, P. J. Maddon, R. A. Koup, J. P. Moore, and W. A. Paxton.** 1996. HIV-1 entry into CD4+ cells is mediated by the chemokine receptor CC-CKR-5. Nature **381:**667–673.
19. **Feng, Y., C. C. Broder, P. E. Kennedy, and E. A. Berger.** 1996. HIV-1 entry cofactor: functional cDNA cloning of a seven-transmembrane, G protein-coupled receptor. Science **272:**872–877.
20. **Fiscus, S. A., V. DeGruttola, P. Gupta, D. A. Katzenstein, W. A. Meyer, M. L. LoFaro, M. Katzman, M. V. Ragni, P. S. Reichelderfer, and R. W. Coombs.** 1995. Human immunodeficiency virus type 1 quantitative cell microculture as a measure of antiviral efficacy in a multicenter clinical trial. J. Infect. Dis. **171:**305–311.
21. **Fouchier, R. A. M., M. Groenink, N. A. Kootstra, M. Tersmette, H. G. Huisman, F. Miedema, and H. Schuitemaker.** 1992. Phenotype-associated sequence variation in the third variable domain of the HIV-1 gp120 molecule. J. Virol. **66:**3183–3187.
22. **Groenink, M., A. C. Andeweg, R. A. Fouchier, S. Broersen, R. C. van der Jagt, H. Schuitemaker, R. E. de Goede, M. L. Bosch, H. G. Huisman, and M. Tersmette.** 1992. Phenotype-associated *env* gene variation among eight related human immunodeficiency virus type 1 clones: evidence for in vivo recombination and determinants of cytotropism outside the V3 domain. J. Virol. **66:**6175–6180.
23. **Groenink, M., R. A. Fouchier, S. Broersen, C. H. Baker, M. Koot, A. B. van't Wout, H. G. Huisman, F. Miedema, M. Tersmette, and H. Schuitemaker.** 1993. Relation of phenotype evolution of HIV-1 to envelope V2 configuration. Science **260:**1513–1516.
24. **Ho, D. D., A. U. Neumann, A. S. Perelson, W. Chen, J. M. Leonard, and M. Markowitz.** 1995. Rapid turnover of plasma virions and CD4 lymphocytes in HIV-1 infection. Nature **373:**123–126.
25. **Hwang, S. S., T. J. Boyle, H. K. Lyerly, and B. R. Cullen.** 1991. Identification of the envelope V3 loop as the primary determinant of cell tropism in HIV-1. Science **253:**71–74.
26. **Japour, A. J., S. A. Fiscus, J. M. Arduino, D. L. Mayers, P. S. Reichelderfer, and D. R. Kuritzkes.** 1994. Standardized microtiter assay for determination of syncytium-inducing phenotypes of clinical human immunodeficiency virus type 1 isolates. J. Clin. Microbiol. **32:**2291–2294.
27. **Javaherian, K., A. J. Langlois, G. J. LaRosa, A. T. Profy, D. P. Bolognesi, W. C. Herlihy, S. D. Putney, and T. J. Matthews.** 1990. Broadly neutralizing antibodies elicited by the hypervariable neutralizing determinant of HIV-1. Science **250:**1590–1593. (Erratum, **251:**13, 1991.)
28. **Koot, M., I. P. Keet, A. H. Vos, R. E. de Goede, M. T. Roos, R. A. Coutinho, F. Miedema, P. T. Schellekens, and M. Tersmette.** 1993. Prognostic value of HIV-1 syncytium-inducing phenotype for rate of CD4+ cell depletion and progression to AIDS. Ann. Intern. Med. **118:**681–688.
29. **Koyanagi, Y., S. Miles, R. T. Mitsuyasu, J. E. Merrill, H. V. Vinters, and I. S. Y. Chen.** 1987. Dual infection of the central nervous system by AIDS viruses with distinct cellular tropisms. Science **236:**819–822.
30. **Kuiken, C. L., J.-J. de Jong, E. Baan, W. Keulen, M. Tersmette, and J. Goudsmit.** 1992. Evolution of the V3 envelope domain in proviral sequences and isolates of human immunodeficiency virus type 1 during transition of the viral biological phenotype. J. Virol. **66:**4622–4627.
31. **Lee, A. B., and T. A. Cooper.** 1995. Improved direct PCR screen for bacterial colonies: wooden toothpicks inhibit PCR amplification. BioTechniques **18:**225–226.
32. **McNearny, T., Z. Hornickova, R. Markham, A. Birdwell, M. Arens, A. Saah, and L. Ratner.** 1992. Relationship of human immunodeficiency virus type 1 sequence heterogeneity to stage of disease. Proc. Natl. Acad. Sci. USA **89:**10247–10251.
33. **Michael, N. L., K. E. Davis, L. D. Loomis-Price, T. C. VanCott, D. S. Burke, R. R. Redfield, and D. L. Birx.** 1996. V3 seroreactivity and sequence variation: tracking the emergence of V3 genotypic variation in HIV-1-infected patients. AIDS **10:**121–129.
34. **Milich, L., B. Margolin, and R. Swanstrom.** 1993. V3 loop of the human immunodeficiency virus type 1 Env protein: interpreting sequence variability. J. Virol. **67:**5623–5634.
35. **Milich, L., B. H. Margolin, and R. Swanstrom.** Patterns of amino acid variability in NSI-like and SI-like V3 sequences and a linked change in the CD4-binding domain of the HIV-1 Env protein. Virology, in press.
36. **Myers, G., B. Korber, B. Foley, K.-T. Jeang, J. W. Mellors, and S. Wain-**

Hobson. 1996. Human retroviruses and AIDS 1996. Los Alamos National Laboratory: Theoretical Biology and Biophysics, Los Alamos, N.Mex.
37. **National Institutes of Health.** 1994. ACTG virology manual for HIV laboratories. National Institutes of Health, Bethesda, Md.
38. **O'Brien, W. A., Y. Koyanagi, A. Namazie, J. Q. Zhao, A. Diagne, K. Idler, J. A. Zack, and I. S. Y. Chen.** 1990. HIV-1 tropism for mononuclear phagocytes can be determined by regions of gp120 outside the CD4-binding domain. Nature **348:**69–73.
39. **Preston, B. D., B. J. Poiesz, and L. A. Loeb.** 1988. Fidelity of HIV-1 reverse transcriptase. Science **242:**1168–1171.
40. **Sabino, E., L.-Z. Pan, C. Chang-Mayer, and A. Mayer.** 1994. Comparison of *in vivo* plasma and peripheral blood mononuclear cell HIV-1 quasispecies to short-term tissue culture isolates: an analysis of *tat* and C2-V3 *env* regions. AIDS **8:**901–909.
41. **Sambrook, J., E. F. Fristch, and T. Maniatis.** 1989. Molecular cloning: a laboratory manual, 2nd ed. Cold Spring Harbor Laboratory Press, Cold Spring Harbor, N.Y.
42. **Schuitemaker, H., M. Koot, N. A. Kootstra, M. W. Dercksen, R. E. Y. de Goede, R. P. Van Steenwijk, J. M. A. Lange, J. K. M. Eeftink-Schattenkerk, F. Miedema, and M. Tersmette.** 1992. Biological phenotype of human immunodeficiency virus type 1 clones at different stages of infection: progression of disease is associated with a shift from monocytotropic to T-cell-tropic virus populations. J. Virol. **66:**1354–1360.
43. **Shioda, T., J. A. Levy, and C. Cheng-Mayer.** 1992. Small amino acid changes in the V3 hypervariable region of gp120 can affect the T-cell-line and macrophage tropism of human immunodeficiency virus type 1. Proc. Natl. Acad. Sci. USA **89:**9434–9438.
44. **Simmons, G., D. Wilkinson, J. D. Reeves, M. T. Dittmar, S. Beddows, J. Weber, G. Carnegie, U. Desselberger, P. W. Gray, R. A. Weiss, and P. R. Clapham.** 1996. Primary, syncytium-inducing human immunodeficiency virus type 1 isolates are dual-tropic and most can use either Lestr or CCR5 as coreceptors for virus entry. J. Virol. **70:**8355–8360.
45. **Tersmette, M., R. A. Gruters, F. de Wolf, R. E. de Goede, J. M. Lange, P. T. Schellekens, J. Goudsmit, H. G. Huisman, and F. Miedema.** 1989. Evidence for a role of virulent human immunodeficiency virus (HIV) variants in the pathogenesis of acquired immunodeficiency syndrome: studies on sequential HIV isolates. J. Virol. **63:**2118–2125.
46. **Tersmette, M., J. M. A. Lange, R. E. Y. de Goede, F. de Wolf, J. K. M. Eeftink-Schattenkerk, P. T. A. Schellekens, R. A. Coutinho, J. G. Huisman, J. Goudsmit, and F. Miedema.** 1989. Association between biological properties of human immunodeficiency virus variants and risk for AIDS mortality. Lancet **i:**983–985.
47. **Veenstra, J., R. Schuurman, M. Cornelissen, A. B. van't Wout, C. A. Boucher, H. Schuitemaker, J. Goudsmit, and R. A. Coutinho.** 1995. Transmission of zidovudine-resistant human immunodeficiency virus type 1 variants following deliberate injection of blood from a patient with AIDS: characteristics and natural history of the virus. Clin. Infect. Dis. **21:**556–560.
48. **Wang, Y.-H., and J. Griffith.** 1991. Effects of bulge composition and flanking sequence on the kinking of DNA by bulged bases. Biochemistry **30:**1358–1363.
49. **Wei, X., S. K. Ghosh, M. E. Taylor, V. A. Johnson, E. A. Emini, P. Deutsch, J. D. Lifson, S. Bonhoeffer, M. A. Nowak, B. H. Hahn, M. S. Saag, and G. M. Shaw.** 1995. Viral dynamics in human immunodeficiency virus type 1 infection. Nature **373:**117–122.
50. **Westervelt, P., D. B. Trowbridge, L. G. Epstein, B. M. Blumberg, Y. Li, B. H. Hahn, G. M. Shaw, R. W. Price, and L. Ratner.** 1992. Macrophage tropism determinants of human immunodeficiency virus type 1 in vivo. J. Virol. **66:**2577–2582.